

## Optical Coherence Tomography for the Middle and Inner Ear

Justus Ilgner, Tino Just, Csaba Farkas, Achim Lenenbach, and Martin Westhofen

---

### Introduction

With the advent of operating microscopes in the early 1950s and the continuous development of prosthetic materials, functional restoration of hearing, whenever impaired sound conduction is the leading phenomenon, became a reliable treatment modality in the hands of otologic surgeons. For diagnostic purposes, a variety of functional tests form the repertoire from which the diagnosis for the underlying disease process is made. However, in most cases the cause for conductive hearing loss can only be concluded indirectly from a variety of audiometric findings. Direct visualization of the pathologic process is one need which has not yet been fully met. At present, magnetic resonance imaging and computed tomography images provide resolutions in the range of 300  $\mu\text{m}$ . CT scans are mostly used to detect bony abnormalities as soft tissue differentiation is limited. Over recent years, Flat Panel CT, Cone Beam CT, and Digital Volume Tomography are about to increase resolution for middle and inner ear structures, but these imaging techniques cannot be used with contrast agents. On the other hand, MRI imaging is undergoing a continuous evolution process with higher field strengths, enabling soft tissue differentiation within middle ear structures for the detection of chronic middle ear inflammation involving epithelial growth, i.e., cholesteatoma. However, MRI scanners with field strengths of 7.5–10 T are required, which are not yet available for clinical routine.

OCT for the middle and inner ear faces considerable advantages as well as challenges: The tympanic membrane is readily accessible in humans, while the penetration of near infrared light

does not require any transduction medium as in ultrasound. Therefore, structures within the air-filled middle ear cavity are readily visible. The imaging process can be noninvasive, and the size of structures under investigation meets the range suitable for OCT. Imaging devices can be built in small, compact units. They can be coupled to existing devices, as the operating microscope or a handheld otoscope, and can be operated by the clinician or operating surgeon himself who can also interpret the results. OCT provides visible results in real-time, making it suitable for quality control, e.g., in the operating theater. The change of refraction index between air and liquid, when facing an open inner ear, e.g., during stapes surgery, is not an obstacle for OCT, as long as image distortion along the  $z$  axis is taken into account and, if necessary, corrected by image processing. On the down side, however, *in vivo* imaging of nonanesthetized subjects can suffer from movement artifacts, which can be overcome by increasing image acquisition rates. Imaging through an intact tympanic membrane can attenuate the signal and create artifacts, if the TM is sclerotic or thickened, making visualization of middle ear structures difficult or impossible. Finally, penetration depth through solid bone is limited, requiring a direct line of sight to the region of interest in most cases. Middle ear ossicles or overhanging parts of the outer ear canal can obstruct the scanning beam. Yet there are numerous approaches considering the use of OCT either as an imaging modality on its own or as an adjunct in functional investigations of the middle ear, which have the potential to widen the diagnostic spectrum of otologists in clinical routine over the next decades.

---

## OCT in Experimental Middle and Inner Ear Imaging: Ex Vivo and In Vivo

Pitris and coworkers [1] were one of the first to apply OCT to middle ear imaging in general. In an *ex vivo* experiment using four human temporal bones from cadavers, they employed a TD-OCT scanner with a probe introduced next to the outer ear canal, in 15 mm distance to the closed tympanic membrane. Acquisition time of one B-image took between 10 and 30 s. While the authors noticed shadowing effects of solid structures, as middle ear ossicles, and resolution loss by the closed tympanic membrane, they were still able to identify and label middle ear structures. They concluded that OCT has the advantage of using air, as well as fluids/soft tissues as a transduction medium, thereby making it suitable for middle ear imaging in real time. Probes could be built compact and adapted to any kind of instrument used in otology.

Just et al. [2–4] specifically aimed to characterize the oval niche and the stapes footplate. In a first experiment, they used an

SD-OCT system producing 1000 A-lines per second, which was coupled to a conventional operating microscope. First results could differentiate layers (bone and cartilage) within the stapes footplate. Furthermore, the elastic suspension of the stapes footplate could be identified, although anatomical variations in some cases, as an overhanging facial nerve, might prevent this. Following stapes perforation by CO<sub>2</sub> laser, the outline of the vestibulum was visualized through the open footplate by OCT. The authors also noted that while working on the open vestibulum, resulting images required depth correction along the *z*-axis, as the refraction index in an air-filled middle ear (1.0) is different from the inner ear filled with fluids, i.e., perilymph and endolymph (1.33).

Subhash and coworkers [5] proposed a system for ultra-high sensitive optical microangiography, which they used to visualize blood flow in the cochlea of mice. Their system is based on an SD-OCT scanner acquiring 47,000 A-scans per second, resulting in high-resolution B-scans at a rate of 300 frames per second. Their system is sensitive for flow velocities between 4.0 μm/s and 30 mm/s, making it suitable for physiological blood flow rates down to capillary level. They were able to create 3D volumetric images of blood flow in the basal, middle, and apical turn of the mouse cochlea, depicting inner ear structures as the modiolus, stria vascularis, Reissner's membrane, and basilar membrane and visualizing blood flow in the stria vascularis in particular using the phase difference between adjacent B-scans. Resolution is sufficiently high in order to subsegment different areas of the cochlea from three-dimensional reconstruction, thereby enabling the measurement of blood flow in different cochlear structures separately.

In another experiment by the same workgroup [6], phase-sensitive SD-OCT was used to detect sound induced motions of middle ear structures, thereby using the SD-OCT system as a middle ear vibrometer. From a human temporal bone cadaver, structural B-scan images were taken and compared to vibrational images visualizing the velocity of different areas of the tympanic membrane as well as of the middle ear ossicles. Using this method, which was applied through the closed tympanic membrane, the authors propose the setup to diagnose different causes of conductive hearing loss directly and noninvasively.

Cho et al. [7] also combined an SD-OCT scanner with a surgical microscope for imaging middle ear and inner ear structures in mice through the closed tympanic membrane. In their experiment, they also created models of different clinical situations, e.g., middle ear effusion, remaining effusion after paracentesis and suction, tympanic membrane perforation, and compared these to OCT imaging results. In their view, the advantage of SD-OCT lies in imaging and 3D image reconstruction of middle ear structures in vivo which is now possible in real-time.

Chang et al. [8] in a recent study were able to use an OCT system to simultaneously visualize sound induced motions of the tympanic membrane and middle ear ossicles in three-dimensional reconstruction of three temporal bones from chinchilla cadavers. They examined pure tone frequencies of 800, 1910, and 3050 Hz. Their OCT system produces 15,000–20,000 A-lines per second, while the number of A-scans divided by the pure tone frequency under examination results in the number of different phases displayed by the system. Sensitivity for tympanic membrane movement was 0.5 nm and 5 nm for the stapes footplate, as all measurements were performed through the closed tympanic membrane. Different motion and phase-related features could be identified for (a) normal middle ear structures, (b) stapes fixation, and (c) interruption of the incudo-stapedial joint. As for future perspectives, the authors see the potential to differentiate between different causes of conductive hearing loss directly in an outpatient setting using their system.

With similar intention, Burkhardt and coworkers [9] presented a Doppler OCT system to analyze human temporal membrane motion by acoustic chirps over a frequency range between 400 Hz and 6400 Hz. They used a Frequency-Domain OCT system with a center wavelength of  $1300 \text{ nm} \pm 160 \text{ nm}$ . Lateral resolution was calculated at  $9 \text{ }\mu\text{m}$  and axial resolution at  $13 \text{ }\mu\text{m}$ . Measuring the tympanic membrane with 512 Motion(M)-scans in  $z$  axis at a rate of 60 kHz over a grid of  $25 \times 25$  points, 8.5 ms were required for one scan to render one full tympanic membrane scan over 625 points within 5.3 s. By means of the setup, tympanic membrane motion showed an increasing complexity and falling amplitude with rising frequency. Resonance frequency of the human tympanic membrane was observed at 1062 Hz, while amplitude maxima were observed to shift over different spots with varying frequency. Their setup, however, employed a human temporal bone model, although the authors see the possibility to adapt it for clinical use with reasonable effort.

---

## OCT in Clinical Middle and Inner Ear Imaging

One of the first to use OCT in clinical settings, Heermann and coworkers [10] coupled a TD-OCT scanner to an operating microscope and used it under sterile conditions while performing microsurgery of the middle ear. They employed the OCT system in B-Mode in five cases of tympanoplasty type III, i.e., restoration of the tympanic membrane, the malleus, the incus, and—in some cases—the stapes suprastructure following chronic inflammation of the middle ear, as well as five cases of stapes surgery, in which the stapes is fixed by a sclerotic change of the elastic ring supporting it to the inner ear capsule. In both operations, OCT was mainly used

to measure the length of the prosthesis which is critical for reestablishing sound transmission in the best possible way. The authors concluded that optical measurement of distances in the inner ear were preferable over mechanical measurement, as the latter always carries the risk of destruction to the remaining middle ear chain, particularly breaking the stapes footplate. The authors stated that B-mode imaging through a closed tympanic membrane were impossible due to methodological restrictions. Although this may apply to cases of tympanosclerosis or extreme scarring, in cases of healthy, semi-transparent tympanic membranes this hypothesis was proven otherwise by later authors.

Djalilian et al. [11, 12] employed a TD-OCT-system in an outpatient setting in order to characterize healthy tympanic membranes and to differentiate these from distinct pathological processes. In 10 patients, they were able to delineate the physiological trilaminar structure of the tympanic membrane with an outer squamous layer, middle fibrous layer, and medial cuboidal epithelium. This trilaminar structure could be differentiated from atrophic areas of the tympanic membrane with only one thin layer visible. Furthermore, hyperkeratosis of the tympanic membrane, a tympanosclerotic plaque, and cholesteatoma could be seen, although in these three cases, penetration depth of the infrared light is limited and therefore prevents further differentiation in depth, as well as judging the extent of chronic inflammatory process as in cholesteatoma. Image acquisition rate was 1 Hz, making it suitable for the practical use in an outpatient department with a total examination time of 3 min for each patient.

In the aforementioned studies by Just et al. [2–4], imaging of the oval window niche in human temporal bones was transferred to an operative setting in eight patients undergoing stapes surgery. In these patients, the sclerotic changes to the elastic suspension of the stapes footplate, as well as the footplate itself were contrasted against their results obtained from healthy temporal bones *ex vivo*. Scanning speed allowed imaging in B-mode in real time, although three-dimensional reconstruction of the data required some image postprocessing and could not be realized in an operative setting. However, scan resolution allowed online characterization of shape and extent of sclerotic changes encountered in otosclerosis patients. As a practical aspect, the use of the SD-OCT scanner extended the total duration of surgery by 5–10 min.

In 2012, Nguyen et al. [13] from S. Boppart's workgroup set out to detect bacterial biofilm attached to the inner layer of the tympanic membrane of patients with chronic otitis media (COM)/otitis media with effusion (OME). The general hypothesis is that bacteria whose number per volume exceeds a certain threshold can produce a thick layer of mucopolysaccharides which is impenetrable by macrophages, lymphocytes, etc. as well as by

antibiotics. Nguyen et al. aimed to detect this layer optically. They used two methods, low coherence interferometry (LCI) and optical coherence tomography, either as a stand-alone method (LCI) or in combination, using a custom built hand-held device similar to an office otoscope. From a total of 20 individuals, 13 patients with clinical signs of COM and seven healthy controls, 18,537 LCI scans and 742 OCT images were taken. Biofilm was defined as a thick and highly scattering signal up to a depth of 400  $\mu\text{m}$  (200  $\mu\text{m}$  average) behind the tympanic membrane, while the TM itself showed two distinct peaks about 90  $\mu\text{m}$  apart, related to the outer and inner epithelial layer. As many LCI scans per ear were taken, the specificity for the presence of biofilm was such that normal ears had a low percentage of abnormal scans (<11 %), while ears with presence of biofilm had an abnormal scan rate of >37 %. Therefore, the authors set the threshold of biofilm diagnosed with LCI/OCT at a rate of abnormal scans of >25 % per ear resulting in a sensitivity of 68 % and specificity of 98 %. According to the authors, the low sensitivity can be explained by patchy areas of biofilm that result in normal and abnormal scans at the same time in one ear.

In a consecutive study [14], the workgroup of Nguyen and Boppart compared the presence of biofilm assessed by OCT to acoustic effects on the tympanic membrane induced by biofilm. They found that in cases with the presence of biofilm confirmed by OCT, tympanic membranes showed certain features of acoustic resistance and power reflectance that could be differentiated from normal tympanic membranes and potentially also from TM in chronic otitis media with effusion. However, the authors also state that three-dimensional reconstruction of OCT images could help identifying the extent of biofilm and its local effects of TM movement, while in this study local effects were difficult to assess as only two-dimensional images were available.

---

## OCT in Conjunction with Other Experimental Methods

McCaughey and coworkers [15] used a TD-OCT scanner to compare the shape of bone ablated by two different lasers, an Er:YAG laser (2940 nm) and a femtosecond laser (1053 nm) *ex vivo*. Other means of characterization were light microscopy and scanning electron microscopy (SEM). Although penetration depth of OCT was extremely limited in bone, the ablation depth was easily quantified as well as ablation margins characterized without mechanically cross-sectioning of the specimen, thereby avoiding preparation artifacts.

The question which thermal alterations affect the perilymph during CO<sub>2</sub> laser stapedotomy was addressed by Just and coworkers in 2010 [16]. In this context of an *ex vivo* experiment, the shape

and thickness of the stapes footplate as well as the shape of the CO<sub>2</sub> laser-induced footplate perforation were addressed. To achieve this, the shape of the footplate was reconstructed three-dimensionally using data from the SD-OCT scanning system described in [2–4]. The OCT data confirmed perforation diameters between 490 and 550 μm with an unevenly shaped “crystallization zone” and evenly shaped, unaffected bone. No significant correlation was found between the thickness of the stapes footplate and the perforation diameter.

Just et al. [17] also examined tympanic membrane movement by using a film patch with integrated strain gauge. In this context, two different types of film patch with integrated strain gauge were attached to tympanic membranes *in vitro*. The SD-OCT system described in [2–4] was employed to (a) assess the thickness of tympanic membranes under investigation *in vitro* and *in vivo* and (b) evaluate whether the film patch was tightly attached to the tympanic membrane surface during pressure changes, leaving no gaps between the membrane and the film patch.

---

## Own Experience

In a research project conducted jointly by the Fraunhofer Institute for Laser Technology (ILT) and the Department of Otorhinolaryngology, Plastic Surgery of the Head and Neck, RWTH Aachen, we aimed to evaluate the use of OCT for otologic diagnosis in an outpatient setting. The objective was to create an additional tool for the otologist to (i) confirm/refine the clinical diagnosis made by otomicroscopy for preoperative patients and to (ii) follow up patients postoperatively for early detection of recurrent disease, e.g., cholesteatoma.

A time-domain OCT system with a low-coherent super luminescent diode light source with a center wavelength of 1310 nm was coupled to the front lens of a microscope via a micromanipulator (Figs. 1 and 2). The micromanipulator allows adjustment of the scan direction and the field of view of about 1 × 1 mm minimum to 2 × 3 mm maximum. The system creates 200 A-lines per second in an  $x/y$  matrix of 100 × 100 scans, resulting in a total scan time of 50 s for one volumetric scan. As the field of view in  $x/y$  direction is variable so is the transverse resolution of the system. The axial resolution is 10 μm, with a comparatively large scan range along the  $z$ -axis of 9 mm. This range was necessary in order to achieve one scan ranging from the tympanic membrane to the medial wall of the middle ear, e.g., the promontory and structures in between (Table 1).

A standard resolution CCD camera was incorporated in the system to monitor areas under scan and to document the clinical



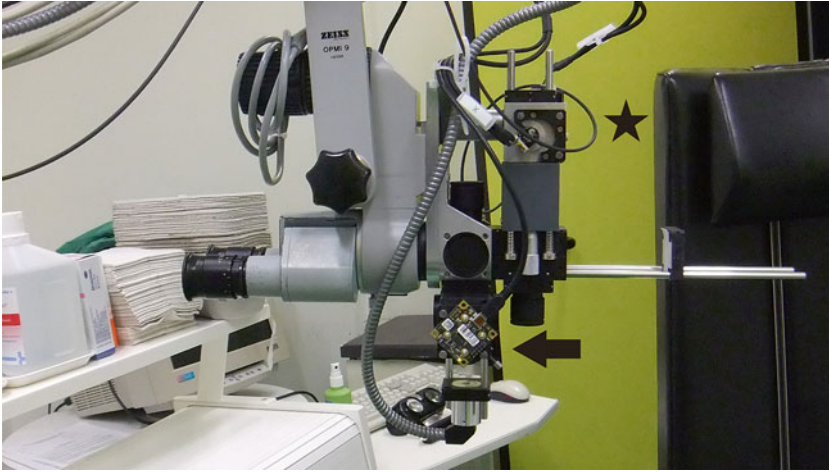


**Fig. 1** Oto-Microscope (Zeiss OPMI9) in outpatient department with micromanipulator attached including  $x/y$  scanner drive (*star*) and CCD camera (*arrow*). The guide rails to the right are attached for calibration purposes only



**Fig. 2** Setup in outpatient department for examination of the *right ear*

aspect as seen through the microscope (Fig. 3). The tympanic membrane, posterior wall of the outer ear canal, and the umbo (tip of the malleus inserting at the center of the tympanic membrane) were always visible and considered as reference structures, while the promontory, round window membrane, long incus process, and stapes suprastructure were regarded as target structures (Fig. 4). The aim was to visualize target structures through an intact



**Table 1**  
**Optical coherence tomography for the middle and inner ear**

Investigator	Year	OCT system	Wavelength	Transverse resolution	Axial resolution	Image acquisition rate	Setting	Material/patients	Purpose
Pitris et al. [1]	2001	TD-OCT	1310 nm $\pm$ 50 nm	10–20 $\mu$ m	15 $\mu$ m	10–30 s for 1 B-frame	Experimental	Four human temporal bones	Feasibility study
Heermann et al. [10]	2002	TD-OCT	975 nm $\pm$ 36 nm	30 $\mu$ m	12 $\mu$ m	200 A-lines/s $\geq$ 1 B-frame/s	Clinical, intraoperative	Ten patients	Distance measurement for stapes/PORP/TORP prosthesis
Djalilian et al. [11, 12]	2008	TD-OCT	1310 nm	10 $\mu$ m	7 $\mu$ m	1 B-frame/s	Clinical, out-patient	Ten patients	Tympanic membrane characterization
Just et al. [2–4]	2009	SD-OCT	830 nm	23 $\mu$ m	12 $\mu$ m	1,000 A-lines/s $\geq$ 1 B-frame/s	Experimental	Five human temporal bones	Oval niche characterization
McCaughey et al. [15]	2009	TD-OCT	1310 nm	<50 $\mu$ m	10–20 $\mu$ m	1 B-frame/s	Experimental	Human bone specimen	Evaluation of Femtosecond laser ablation of bone
Just et al. [16]	2010	SD-OCT	830 nm	23 $\mu$ m	12 $\mu$ m	1000 A-lines/s $\geq$ 1 B-frame/s	Experimental	Human stapes	Thermographic measurement of heat deposition in CO <sub>2</sub> laser stapelotomy, stapes and perforation morphology
Subhash et al. [5]	2011	SD-OCT	1300 nm $\pm$ 28 nm	16 $\mu$ m	13 $\mu$ m	47,000 A-lines/s $\geq$ 300 B-frames/s	Experimental	Mouse cochlea	Vascular imaging and blood flow velocity measurement

**Table 1**  
(continued)

Investigator	Year	OCT system	Wavelength	Transverse resolution	Axial resolution	Image acquisition rate	Setting	Material/patients	Purpose
Just et al. [17]	2011	SD-OCT	840 nm	24 $\mu\text{m}$	12 $\mu\text{m}$	1000 A-lines/s $\geq 1$ B-scan/s	Experimental	Three human temporal bones	Tympanic membrane characterization, attachment of film strain gauge
Subhash et al. [6]	2012	PS-SD-OCT	1300 nm $\pm 28$ nm	16 $\mu\text{m}$	13 $\mu\text{m}$		Experimental	Two human temporal bones	Vibrational measurement of ossicular chain under 500 Hz/65 dB stimulus
Nguyen et al. [13]	2012	SD-OCT and LCI	830 nm $\pm 70$ nm (OCT) 940 nm $\pm 70$ nm (LCI)	30 $\mu\text{m}$ (LCI)	3.1 $\mu\text{m}$ (OCT) 4 $\mu\text{m}$ (LCI)	70,000 A-lines/s $\geq$ 1000 scans/s (LCI) 70 B-frames/s (OCT)	Clinical, out-patient	Four healthy individuals, sixteen patients	Bacterial biofilm detection on tympanic membrane
Nguyen et al. [14]	2013	SD-OCT	830 nm $\pm 70$ nm		3.1 $\mu\text{m}$	70,000 A-lines/s $\geq 70$ B-frames/s (OCT)	Clinical, out-patient	One healthy individual, five patients	Assessment of acoustic effects of bacterial biofilm on human TM
Chang et al. [8]	2013	PS-SD-OCT	1220 nm–1350 nm tunable	25 $\mu\text{m}$	12 $\mu\text{m}$	18,000 A-lines/s	Experimental	Three chinchilla temporal bones	Vibrational measurement of ossicular chain physiological and pathological conditions
Cho et al. [7]	2014	SD-OCT	870 nm $\pm 65$ nm	30.2 $\mu\text{m}$	8.7 $\mu\text{m}$		Experimental	Five mice	Middle ear characterization under physiological and pathological conditions

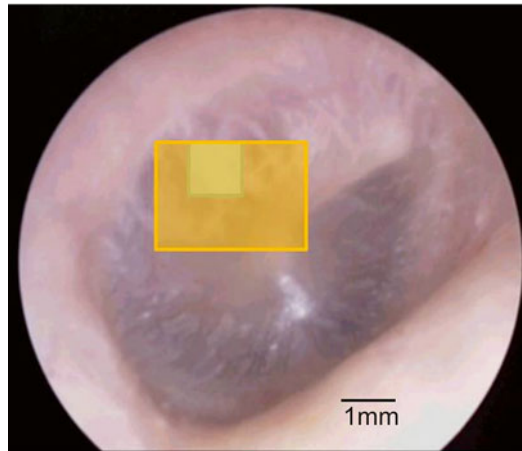


**Fig. 3** OCT scan area varying from  $1 \times 1$  mm (*light green square*) up to  $2 \times 3$  mm (*yellow rectangle*) in relation to tympanic membrane size (*right ear*)

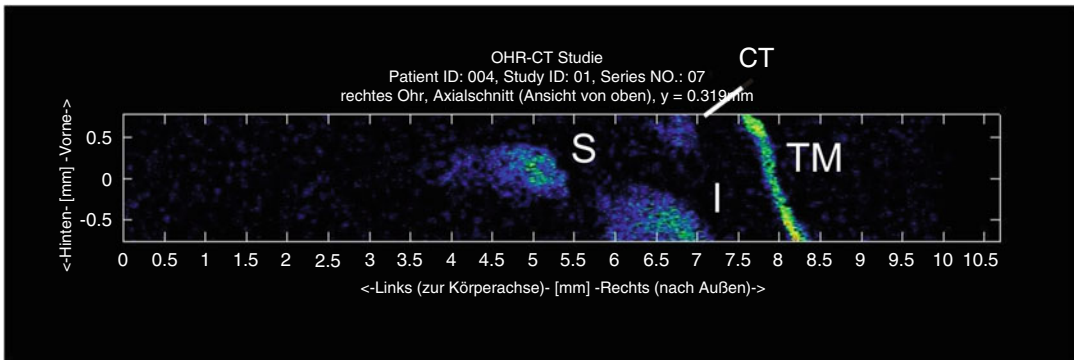


**Fig. 4** OCT scan of a healthy right ear (outer ear canal to the right) showing outlines of tympanic membrane (TM), chorda tympani (CT), long incus process (I), and stapes head (S) (Image by C. Farkas and A. Lenenbach, Fraunhofer Institute of Laser Technology, Aachen)

tympanic membrane in 18 healthy individuals and 13 patients with varying pathology. In 56 scans of healthy individuals, the promontory could be identified in 35 scans, the long incus process in 21, round window membrane in 8, and stapes suprastructure in 4. Of 26 scans performed in patients, the identification of aforementioned structures was possible in 3, 1, 3, and 0 scans, respectively. Although results in patients seem disappointing considering the identification of structures for the middle ear, it has to be mentioned that the anatomy was largely altered by the underlying pathological process itself and by the following surgery. Secondly, although thickened tympanic membranes following tympanoplasty are absorbing and scattering most of the infrared light, alterations in the near field close to the tympanic membrane could be seen (Figs. 5 and 6).

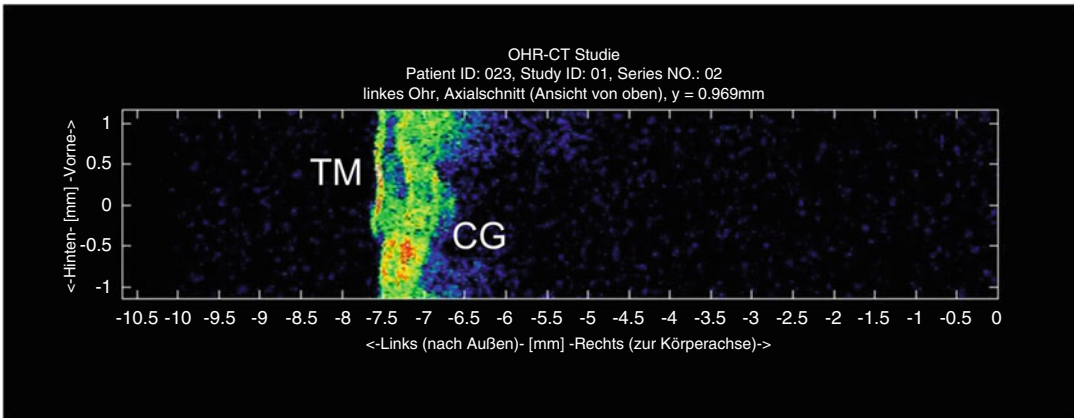


**Fig. 5** OCT scan of a left ear (outer ear canal to the *left*) showing a tympanoplasty type I (i.e., tympanic membrane repair only) in postoperative follow-up. Tympanic membrane (TM) with edge of former perforation, supported by cartilage graft (CG) (Image by C. Farkas and A. Lenenbach, Fraunhofer Institute of Laser Technology, Aachen)

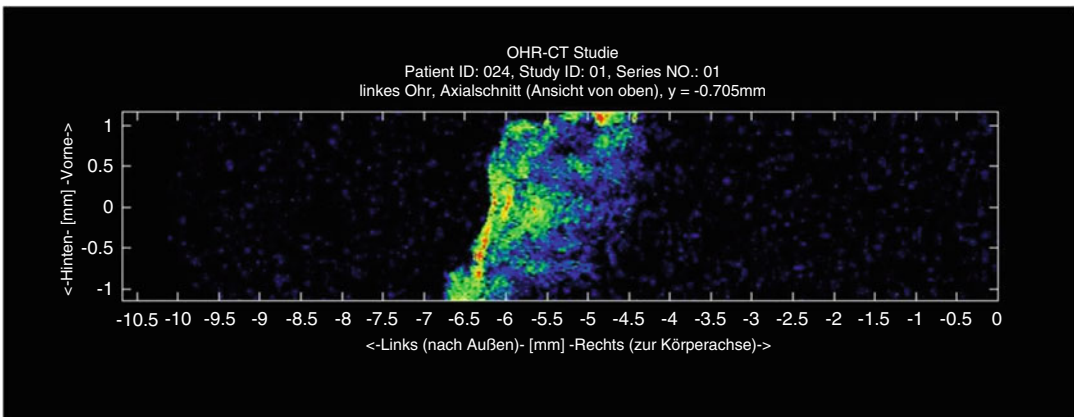


**Fig. 6** OCT scan of a left ear (outer ear canal to the *left*) showing a pars tensa cholesteatoma: Note the cloudy structure of >2 mm thickness (Image by C. Farkas and A. Lenenbach, Fraunhofer Institute of Laser Technology, Aachen)

With scanning speed of 200A-lines per second, patients had to keep still for 50 s in order to reduce motion-related artifacts as good as possible. On the other hand, patients readily accepted the use of OCT, as the examination was conducted within the normal course of otomicroscopy and did not create any discomfort whatsoever. Consequently, OCT has the potential to become a powerful imaging modality in the hands of the otologist, bridging the gap between experimental research and everyday clinical use.

## Acknowledgements

This study was conducted jointly by Dipl.-Ing. Csaba Farkas and Dr.-Ing Achim Lenenbach, both Fraunhofer Institute for Laser Technology (ILT), Aachen, and the author. OCT system and equipment including custom-built scanner, micromanipulator, and CCD monitoring camera were built, adjusted, and operated by the ILT, while examination of healthy individuals as well as patients was performed by the author.

## References

1. Pitris C, Saunders KT, Fujimoto JG, Brezinski ME. High-resolution imaging of the middle ear with optical coherence tomography: a feasibility study. *Arch Otolaryngol Head Neck Surg.* 2001;127:637–42.
2. Just T, Lankenau E, Hüttmann G, Pau HW. Intraoperative application of optical coherence tomography (OCT) for visualization of the oval window niche. *Laryngorhinootologie.* 2009;88:168–73.
3. Just T, Lankenau E, Hüttmann G, Pau HW. Optical coherence tomography of the oval window niche. *J Laryngol Otol.* 2009;123:603–8.
4. Just T, Lankenau E, Hüttmann G, Pau HW. Optical coherence tomography in middle ear surgery. *HNO.* 2009;57:421–7.
5. Subhash HM, Davila V, Sun H, Nguyen-Huynh AT, Shi X, Nuttall AL, Wang RK. Volumetric in vivo imaging of microvascular perfusion within the intact cochlea in mice using ultra-high sensitive optical microangiography. *IEEE Trans Med Imaging.* 2011;30:224–30.
6. Subhash HM, Nguyen-Huynh A, Wang RK, Jacques SL, Choudhury N, Nuttall AL. Feasibility of spectral-domain phase-sensitive optical coherence tomography for middle ear vibrometry. *J Biomed Opt.* 2012;17:060505.
7. Cho NH, Jang JH, Jung W, Kim J. In vivo imaging of middle-ear and inner-ear microstructures of a mouse guided by SD-OCT combined with a surgical microscope. *Opt Express.* 2014;22(8):8985–95.
8. Chang EW, Cheng JT, Rösli C, Kobler JB, Rosowski JJ, Yun SH. Simultaneous 3D imaging of sound-induced motions of the tympanic membrane and middle ear ossicles. *Hear Res.* 2013;304:49–56. doi:10.1016/j.heares.2013.06.006.
9. Burkhardt A, Kirsten L, Bornitz M, Zahnert T, Koch E. Investigation of the human tympanic membrane oscillation ex vivo by Doppler optical coherence tomography. *J Biophotonics.* 2014;7:434–41.
10. Heermann R, Hauger C, Issing PR, Lenarz T. Application of optical coherence tomography (OCT) in middle ear surgery. *Laryngorhinootologie.* 2002;81:400–5.
11. Djalilian HR, Ridgway J, Tam M, Sepehr A, Chen Z, Wong BJ. Imaging the human tympanic membrane using optical coherence tomography in vivo. *Otol Neurotol.* 2008;29:1091–4.
12. Djalilian HR, Rubinstein M, Wu EC, Naemi K, Zardouz S, Karimi K, Wong BJ. Optical coherence tomography of cholesteatoma. *Otol Neurotol.* 2010;31:932–5.
13. Nguyen CT, Jung W, Kim J, Chaney EJ, Novak M, Stewart CN, Boppart SA. Noninvasive in vivo optical detection of biofilm in the human middle ear. *Proc Natl Acad Sci USA.* 2012;109:9529–34.
14. Nguyen CT, Robinson SR, Jung W, Novak MA, Boppart SA, Allen JB. Investigation of bacterial biofilm in the human middle ear using optical coherence tomography and acoustic measurements. *Hear Res.* 2013;301:193–200.
15. McCaughey RG, Sun H, Rothholtz VS, Juhasz T, Wong BJ. Femtosecond laser ablation of the stapes. *J Biomed Opt.* 2009;14:024040.
16. Just T, Specht O, Ovari A, Langnau E, Schmidt W, Pau HW. Thermographic investigations during stapedotomy using a CO<sub>2</sub> laser. *Laryngorhinootologie.* 2010;89:549–55.
17. Just T, Zehlicke T, Specht O, Sass W, Punke C, Schmidt W, Lankenau E, Behrend D, Pau HW. Detection of tympanic membrane movement using film patch with integrated strain gauge, assessed by optical coherence tomography: experimental study. *J Laryngol Otol.* 2011;125:467–73.